Black Sea Journal of Engineering and Science
doi: 10.34248/bsengineering.1977492

Open Access Journal
e-ISSN: 2619 – 8991

Research Article
Volume 9 - Issue 5: 2835-2843 / September 2026

EMPIRICAL MASS-RETENTION MODELING, IMAGE-BASED SURFACE TEXTURE ANALYSIS AND COLOR EVALUATION IN VEGETABLE RETANNING OF WET-BLUE LEATHER

Şükrü ÖMÜR[1]*

[1]*Aydın Adnan Menderes University, Aydın Vocational School, Department of Fashion Design, 09010, Aydın, Türkiye*

Abstract: Vegetable retanning modifies the surface, mass-retention and initial color-difference characteristics of wet-blue leather, but dosage selection is still commonly based on practical experience rather than quantitative process descriptors. This study developed a low-cost empirical screening framework for wet-blue bovine leather retanned with mimosa, quebracho and their 50:50 binary mixture at pH 4.0 and pH 5.5. Forty initial tannin dosage levels between 0.5 and 20 g/L were evaluated. Because equilibrium bath concentration was not measured, tannin uptake was expressed only as gravimetric dry weight gain, and fitted curves were interpreted as initial-dosage-based empirical responses rather than thermodynamic adsorption isotherms. Initial color response was evaluated using CIEDE2000 color difference, while digital surface images were analyzed using gray-level co-occurrence matrix descriptors and Surface Roughness Entropy. Quebracho at pH 4.0 displayed a bounded mass-retention trend associated with increased two-dimensional image regularity and reduced entropy. Mimosa at pH 5.5 displayed sustained mass accumulation accompanied by localized image-texture heterogeneity. Across the tested range, mimosa produced lower initial color-difference values than the other tannin systems, while the binary mixture showed intermediate behavior. The combined gravimetric, colorimetric and image-based approach provides a practical non-destructive screening strategy for comparing vegetable retanning conditions. The findings should be interpreted as comparative process trends and should be validated in future work by bath exhaustion monitoring, shrinkage temperature, standardized physical tests and spatially calibrated imaging.

Keywords: Vegetable retanning, Gravimetric mass retention, Surface texture, CIEDE2000, Non-destructive evaluation, Wet-blue leather

***Corresponding author:** Aydın Adnan Menderes University, Aydın Vocational School, Department of Fashion Design, 09010, Aydın, Türkiye
E mail: sukru.omur@adu.edu.tr (Ş. ÖMÜR)
Şükrü ÖMÜR https://orcid.org/0000-0002-7887-722X

Received: June 23, 2026
Accepted: August 28, 2026
Published: September 15, 2026

Cite as: Ömür, Ş. (2026). Empirical mass-retention modeling, image-based surface texture analysis and color evaluation in vegetable retanning of wet-blue leather. *Black Sea Journal of Engineering and Science,* 9(5), 2835-2843.

1. Introduction

Vegetable retanning is a critical stage in wet-blue leather processing because it influences the final structural and aesthetic attributes of the material, including handle, grain tightness, surface uniformity, fullness perception and color. These effects are governed by collagen chemistry, tannin structure, bath pH and post-tanning process conditions (Venter et al., 2012; Covington and Wise, 2019). Condensed tannin extracts, such as mimosa (Acacia mearnsii) and quebracho (Schinopsis lorentzii), are widely used in leather manufacture because of their practical ability to modify collagen-associated properties and because they support more sustainable chemical profiles than many synthetic alternatives (Balasubramanian et al., 2017; Nurichsanto et al., 2023; Wilson et al., 2023).

Despite extensive industrial use, tanners frequently guide retanning recipes and dosage selection by empirical practice rather than by quantitatively structured relationships between applied dosage and measurable outcomes. Conventional evaluation often relies on tactile assessment and end-point appearance, whereas quantitative descriptors linking dosage-dependent deposition to surface morphology, gravimetric retention, physical stability and color performance remain less frequently reported (Balasubramanian et al., 2017; Covington and Wise, 2019). This gap supports the development of complementary low-cost analytical frameworks that can be used alongside established physical and spectroscopic quality-control methods.

Image-based surface analysis offers a practical and low-cost approach for quantifying leather surface morphology. Texture features derived from the gray-level co-occurrence matrix (GLCM), originally formalized for statistical texture classification, can capture spatial patterns related to surface regularity, while Surface Roughness Entropy (SRE) provides an additional statistical descriptor of local gray-level variability based on entropy computed from normalized co-occurrence distributions (Haralick et al., 1973; Baraldi and Parmiggiani, 1995; Sabeenian and Dinesh, 2011;

This work is licensed (CC BY-NC 4.0) under Creative Commons Attribution 4.0 International License

Varghese et al., 2020). In this study, these metrics were adapted as comparative two-dimensional image descriptors; they are not treated as direct measures of three-dimensional physical roughness, bulk fullness, shrinkage stability or chemical tanning efficiency.

Initial color response was assessed using the CIEDE2000 (Delta E00) metric because of its use in color-difference studies (Raggi and Barbiroli, 1993). Nevertheless, recent color-science literature has shown that CAM16-UCS can provide improved perceptual uniformity in many complex color-difference datasets and may outperform older color-difference models under broader viewing and color-space conditions (Li et al., 2017; Luo et al., 2023; Basova et al., 2024). For this reason, Delta E00 is used here as a comparative industrial benchmark for initial color difference, while CAM16-UCS is identified as a necessary extension for future work.

In adsorption-focused studies, Langmuir and Freundlich models are traditionally used to describe equilibrium relationships between solid-phase uptake and residual bath concentration (Ce), and their parameters are meaningful only when the equilibrium phase relationship is experimentally measured (Qiu et al., 2009; Bbumba et al., 2024). In the present study, Ce was not measured; therefore, the fitted curves do not represent thermodynamic adsorption isotherms and should not be interpreted as adsorption capacity, binding affinity or equilibrium saturation. Instead, gravimetric dry mass retention provides an experimentally accessible indicator of total mass deposition on the leather substrate, which may include both chemical interaction and physical deposition.

Accordingly, the objective of this study was to establish a comparative empirical framework for vegetable retanning of wet-blue leather by relating gravimetric mass retention to applied initial dosage (C0) and correlating it with surface texture evolution and color performance. Mimosa, quebracho, and their binary mixture were evaluated under controlled pH conditions using gravimetric mass retention, GLCM-derived texture descriptors, SRE, and CIEDE2000 (Delta E00). The framework is intended as a practical screening tool for textile and leather engineering applications under industrial constraints, not as a substitute for shrinkage temperature, ISO physical tests, spectroscopic bath monitoring, or NIR/PCA-based process control.

2. Materials and Methods

2.1. Materials

Wet-blue leather samples obtained from the same bovine hide and shaved to a standard thickness of 1.2 ± 0.1 mm were used as substrates. Commercial mimosa (Acacia mearnsii) and quebracho (Schinopsis lorentzii) extracts were used as received, together with their 50:50 binary mixture by dry weight. The retained experimental record does not include a supplier certificate specifying commercial grade, sulfitation status or other chemical modification of the extracts. Therefore, the dosage-retention trends are interpreted as responses of the tested commercial materials and should not be generalized to all ordinary or sulfited mimosa and quebracho products without additional chemical specification. All chemicals used for pH adjustment, including formic acid and sodium bicarbonate, were of analytical grade. Distilled water was used for all retanning baths and rinsing procedures. Prior to dosing, the commercial extracts were used directly from their original containers without additional drying, purification, grinding or chemical pretreatment.

2.2. Experimental Design and Retanning Procedure

Leather pieces were cut to an initial dry mass of 5.0 ± 0.2 g. Retanning experiments were performed at a constant bath volume of 400 mL in glass vessels for 8 h at 25 ± 1 °C under mixing to support bath homogeneity.

Two target pH conditions were investigated: pH 4.0 adjusted with formic acid and pH 5.5 adjusted with sodium bicarbonate solution. The available experimental record does not include the exact acid/base concentration, dosing volumes, pH-meter model, or calibration log. Therefore, pH should be interpreted as a controlled target condition within the experimental design rather than as a fully auditable process-control parameter.

The initial tannin dosage was defined as the initial bath concentration (C0, g/L) of the tannin solution. The dosage ranged from 0.5 to 20 g/L across 40 concentration levels, with denser spacing at lower concentrations and wider spacing at higher concentrations. For each tannin system (mimosa, quebracho, and mixture) and pH condition, experiments were conducted in triplicate (n = 3). At the end of the 8 h contact time, fixation was performed in the same bath by lowering the pH to approximately 3.8 using formic acid (Figure 1).

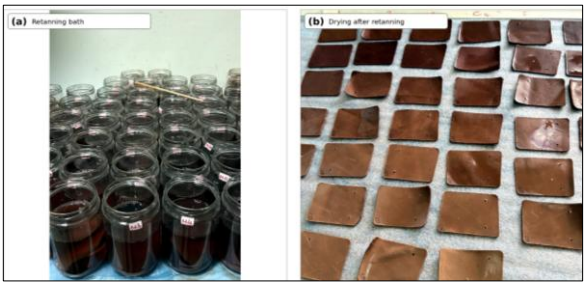


Figure 1. Experimental workflow of the vegetable retanning procedure: (a) immersion of wet-blue leather samples in tannin-containing retanning baths; (b) air-drying of retanned leather samples after fixation and rinsing.

2.3. Gravimetric Uptake and Mass-Retention Calculation

Tannin uptake was quantified exclusively by gravimetric determination of dry mass retention. After retanning and fixation, leather pieces were thoroughly rinsed with distilled water to remove loosely bound material and air-

dried at 25 °C to constant mass. Constant mass was defined as a difference of <0.01 g between two consecutive weighings (equation 1).

$$\text{Weight gain (\%)} = \left[\left(m_{after}\text{-}m_{before}\right)/m_{before}\right]\times 100 \quad (1)$$

where m_{before} is the initial constant dry mass before retanning and m_{after} is the final constant dry mass after retanning and drying. Because shrinkage temperature (Ts), ISO 2420 apparent density and compression-resilience measurements were not performed, gravimetric weight gain is interpreted as mass retention/deposition rather than direct proof of tanning stability or bulk fullness. In future work, Ts should be determined according to ISO 3380, while apparent density and mass per unit area should be determined according to ISO 2420 (International Organization for Standardization, 2015; International Organization for Standardization, 2017).

2.4. Color Measurement

Color was measured using a portable spectrophotometer (Linshang LS170). The CIE L*, a* and b* coordinates were recorded under D65 illumination with a 10° observer angle. Three measurements were taken at different locations on each sample and averaged. The color difference relative to the untreated control was reported as CIEDE2000 (Delta E00), which remains useful for comparability with established industrial color-difference studies (Raggi and Barbiroli, 1993; Luo et al., 2023).

CIEDE2000 was retained to maintain comparability with established leather and industrial color-difference studies. However, because newer uniform color spaces such as CAM16-UCS have shown strong performance in recent color-difference evaluations, the Delta E00 results should be interpreted as comparative initial color-difference values rather than as the final perceptual color model for textured leather surfaces (Li et al., 2017; Luo et al., 2023; Basova et al., 2024). The term initial color consistency is used to avoid implying lightfastness, UV-aging resistance or long-term initial color consistency, none of which was measured in this study.

2.5. Image Acquisition and Surface Texture Analysis

Leather surfaces were imaged under standardized conditions to minimize lighting variability. Images were captured using a DSLR camera with macro capability under stable illumination, converted to 8-bit grayscale, and cropped to a 512 × 512 px region of interest (ROI).

Texture features were extracted using GLCM analysis. GLCMs were computed at a pixel displacement distance of d = 1 and averaged over four angular directions: 0°, 45°, 90° and 135°. In vector form, the corresponding pixel offsets were (1,0), (1,1), (0,1) and (-1,1). Standard GLCM descriptors, including contrast, correlation, homogeneity and energy, were calculated. SRE was computed as Shannon entropy derived from the normalized GLCM distribution (Haralick et al., 1973; Baraldi and Parmiggiani, 1995; Sabeenian and Dinesh, 2011). Energy and entropy were not treated as independent physical measurements; rather, their expected inverse tendency was used cautiously as a consistency check for changes in gray-level order and disorder within the same imaging protocol (Figure 2).

The pixel-to-mm calibration was not available in the archived image metadata. Therefore, the image-derived descriptors should be interpreted as internally comparable metrics within the standardized imaging setup, not as absolute roughness measurements transferable across cameras, lenses or magnification settings without recalibration. This limitation is especially important if the framework is transferred to industrial imaging systems, because GLCM features are sensitive to quantization, displacement distance, angular selection and spatial scaling (Haralick et al., 1973; Baraldi and Parmiggiani, 1995).

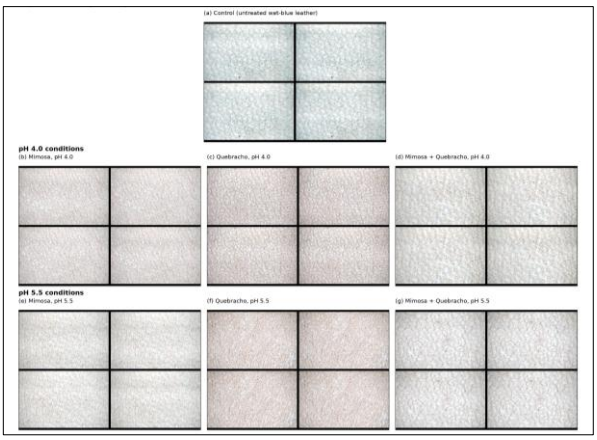


Figure 2. Representative digital surface images used for GLCM- and SRE-based image-processing analysis.

2.6. Statistical Analysis and Empirical Modeling

Analyses were performed using Python (NumPy/Pandas and standard scientific libraries). Pearson correlation coefficients (r) were used to evaluate relationships among gravimetric mass retention, texture metrics (GLCM descriptors and SRE), and Delta E00 values. Because the manuscript dataset does not include a complete inferential output for all pH and agent comparisons, the pH-dependent divergences are interpreted primarily as descriptive empirical trends rather than formal hypothesis-tested effects.

To summarize the relationship between gravimetric mass retention and initial dosage (C0), two neutral mathematical curve forms were used: (i) a bounded-response function to describe curves approaching a plateau-like shape within the tested dosage range and (ii) an empirical power-function to describe sustained dosage-dependent growth. These curve forms are mathematically analogous to commonly used adsorption expressions, but because Ce was not measured, their parameters are descriptive model coefficients rather than thermodynamic adsorption parameters (Qiu et al., 2009; Bbumba et al., 2024). Terms such as plateau-like or sustained response therefore refer only to the empirical

C0-weight-gain relationship.

The complete concentration-level datasets used for curve fitting and color-effectiveness calculations are provided as Supplementary Data S1. The dataset includes tannin content, gravimetric weight gain, Delta E00 and calculated color-effectiveness values for each retanning agent and pH condition.

3. Results

3.1. Empirical Dose-Response of Gravimetric Mass Retention

Tannin deposition was quantified exclusively by gravimetric dry mass retention (weight gain %). Because the equilibrium bath concentration (Ce) was not monitored, the analysis focused on empirical dose-response behavior linking applied initial dosage (C0, g/L) to measured weight gain. The fitted curves are used only to summarize data trends and are not interpreted as thermodynamic isotherms, adsorption capacities, or binding affinities.

The complete raw datasets underlying the dose-response curves, color-difference evaluation and color-effectiveness calculations are provided in Supplementary Data S1.

3.1.1. Quebracho at pH 4.0: Bounded empirical response

For quebracho at pH 4.0, the gravimetric response increased steeply at low dosages and gradually approached a plateau-like shape at higher C0 values. This trend was summarized by a bounded-response fit (R^2 = 0.825), indicating diminishing marginal weight gain at elevated dosages within the tested range (Figure 3). Because extract grade and sulfitation status were not certified in the retained record, the observed trend should be attributed only to the tested commercial quebracho material.

Texture analysis supported an image-based surface-regularity interpretation. Increasing dosage was associated with increased GLCM homogeneity and decreased SRE, consistent with a more ordered two-dimensional grayscale texture under acidic conditions. This interpretation remains strictly image-based; it does not demonstrate three-dimensional physical roughness reduction, equilibrium adsorption or chemical tanning stability.

3.1.2. Mimosa at pH 5.5: sustained empirical power-function trend

In contrast, mimosa at pH 5.5 showed a continuously increasing gravimetric response across the investigated dosage range without a clear plateau. The trend was summarized by an empirical power-function fit (R^2 = 0.755), reflecting sustained dosage-driven mass retention under the tested conditions (Figure 4). Because the commercial modification status of the extract was not certified, this behavior is reported as an empirical response of the tested mimosa material rather than as a universal characteristic of all mimosa extracts.

Compared with quebracho at pH 4.0, the mimosa pH 5.5 system exhibited more localized microtexture variability, as evidenced by a modest increase in SRE and a smaller increase in homogeneity with increasing dosage. This pattern is interpreted as localized two-dimensional surface-texture heterogeneity rather than direct evidence of bulk filling, shrinkage stability, physical roughness change or structural fullness.

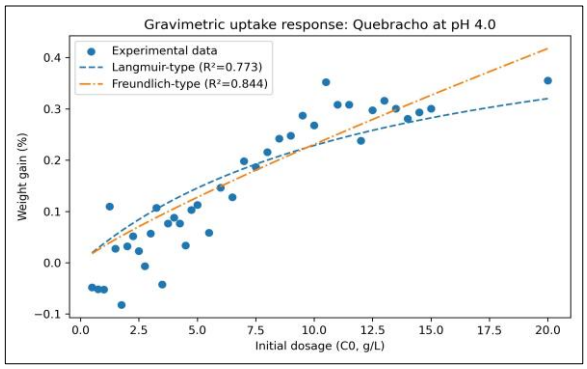


Figure 3. Empirical bounded/power-function dose-response fit for Quebracho at pH 4.0

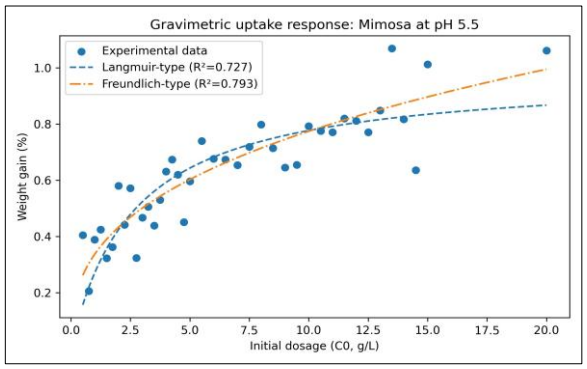


Figure 4. Empirical bounded/power-function dose-response fit for Mimosa at pH 5.5.

3.1.3. Comparative pH-dependent gravimetric responses

A comparative view of the gravimetric responses across agents and pH conditions highlights a clear pH-dependent divergence in the empirical deposition behavior. Quebracho at pH 4.0 tended toward a bounded response accompanied by an image-based increase in surface regularity, whereas mimosa at pH 5.5 demonstrated sustained accumulation with more heterogeneous two-dimensional surface-texture development at higher dosages (Figure 5). These comparisons emphasize that higher mass retention does not correspond to a single surface outcome; instead, dosage-dependent mass retention interacts with pH and tannin type to yield distinct image-derived textural responses.

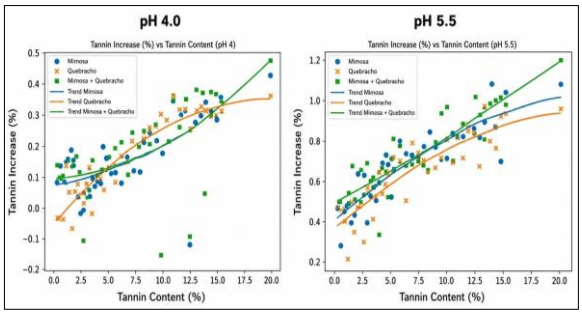


Figure 5. Comparative gravimetric mass retention under pH 4.0 and pH 5.5 conditions.

3.2. Initial Color-Difference Response

The overall optical performance of the leather surface, defined by the color difference (Delta E00) relative to the untreated control, was evaluated alongside gravimetric uptake under varying pH conditions (Tables 1 and 2).

Under pH 4.0 conditions, mimosa produced the lowest mean color difference, indicating lower initial color deviation relative to the untreated control among the tested systems. In contrast, quebracho and the binary mixture exhibited higher initial color deviation. These results should not be interpreted as lightfastness or long-term initial color consistency because no UV-aging or accelerated weathering test was performed.

Table 1. Summary of leather retanning parameters under pH 4.0 conditions (n = 40 per agent)

Group	Tannin uptake (weight gain %, mean ± SD)	Color difference (Delta E00, mean ± SD)
Quebracho	0.149 ± 0.132	20.931 ± 3.294
Mimosa	0.158 ± 0.142	16.335 ± 1.017
Mixture	0.150 ± 0.125	20.069 ± 2.163

Table 2. Summary of leather retanning parameters under pH 5.5 conditions (n = 40 per agent)

Group	Tannin uptake (weight gain %, mean ± SD)	Color difference (Delta E00, mean ± SD)
Quebracho	0.678 ± 0.208	16.911 ± 1.561
Mimosa	0.635 ± 0.201	15.131 ± 2.079
Mixture	0.582 ± 0.193	17.092 ± 1.849

When pH increased to 5.5, gravimetric mass retention increased across all groups and coincided with a general decrease in Delta E00. Based on the concentration-level dataset, mimosa maintained the lowest mean initial color difference at both pH levels within the tested range. However, because color was evaluated only with Delta E00 immediately after processing, these findings should be considered comparative initial color-consistency trends and should be verified with CAM16-UCS and lightfastness or aging tests in future work (Figure 6).

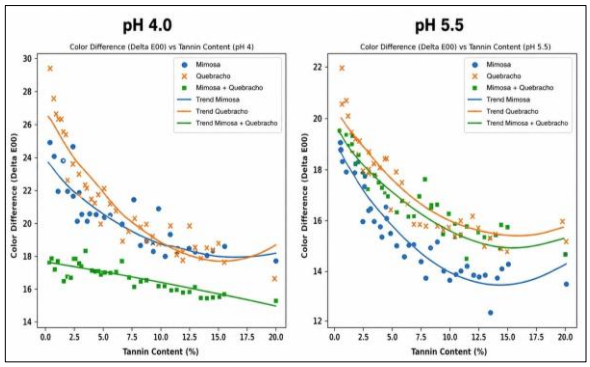


Figure 6. Comparison of agents' color difference (Delta E00) under pH 4.0 and pH 5.5 conditions.

The mixture groups (quebracho + mimosa) demonstrated less consistent initial color responses than mimosa alone. These optical results indicate that pure mimosa offered lower initial color difference under the investigated conditions, although broader validation with additional color models, replicate batches and aging/lightfastness tests is required before any claim of initial color consistency can be made (Figure 7).

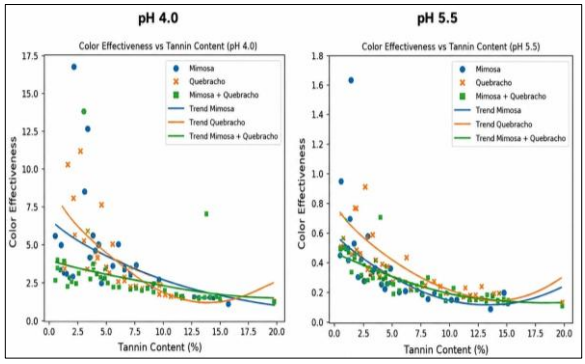


Figure 7. Comparison of agents' color response effectiveness under pH 4.0 and pH 5.5 conditions.

3.3. Surface Texture Evolution from Imaging

Digital image analysis provided objective quantification of changes in two-dimensional surface-image morphology. GLCM descriptors, including homogeneity, captured trends in gray-level spatial regularity, while SRE served as a complementary indicator of gray-level distribution complexity. Because GLCM energy and entropy often vary inversely, they were interpreted together as mutually informative image descriptors rather than as independent physical roughness measurements. These metrics should not be interpreted as direct measures of thickness increase, apparent density, compression-resilience, shrinkage temperature, three-dimensional roughness or bulk fullness.

Representative comparisons between the lowest (0.5 g/L) and highest (20 g/L) dosage conditions illustrated distinct visual and numerical image-texture outcomes (Figure 8). For quebracho at pH 4.0, increasing homogeneity and decreasing SRE supported a progressive image-based surface-regularity tendency.

For mimosa at pH 5.5, the modest increase in SRE indicated localized two-dimensional surface-texture heterogeneity rather than direct evidence of bulk filling or physical roughness change.

Quebracho pH 4.0: At low initial dosage, the sample exhibited high SRE (5.98) and low homogeneity (0.26), indicating a relatively irregular image-texture baseline. At high initial dosage, SRE decreased to 5.52 and homogeneity increased to 0.34. This response should be interpreted as image-based surface regularization under acidic conditions, not as direct physical profilometry evidence.

Mimosa pH 5.5: At low initial dosage, the system began with SRE = 5.55 and homogeneity = 0.34. At high dosage, SRE increased to 5.61 and homogeneity decreased to 0.32. This indicates localized image-texture heterogeneity associated with sustained mass retention. It should not be interpreted as proof of chemical tanning efficacy, physical roughness change or physical fullness without Ts, ISO physical measurements and three-dimensional or calibrated microscopic surface validation.

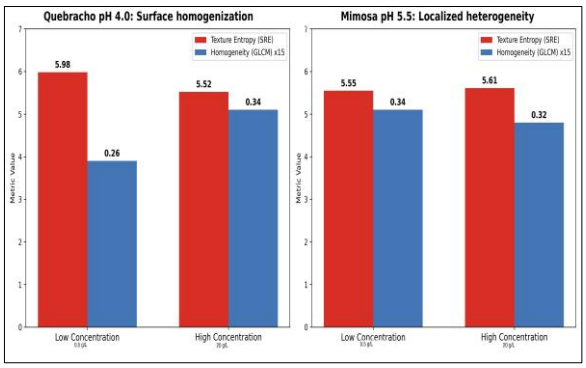


Figure 8. Morphological comparison of lowest and highest tannin dosages based on SRE and GLCM homogeneity

3.4. Combination Analysis

The mimosa-quebracho (50:50) system exhibited intermediate behavior in gravimetric retention and texture response. Although weight gain increased with dosage, the mixture did not replicate the full bounded response of quebracho at pH 4.0 or the sustained power-function response of mimosa at pH 5.5.

The mixed system produced a moderate textural response at both pH levels. A slight positive correlation ($r \approx +0.20$) was observed between dosage and homogeneity. Compared with pure quebracho ($r = +0.68$), the lower homogeneity correlation for the mixture suggests interaction between deposition behaviors; however, this should not be treated as proof of competitive adsorption because equilibrium bath concentrations, extract modification status and molecular-level binding data were not measured (Figure 9).

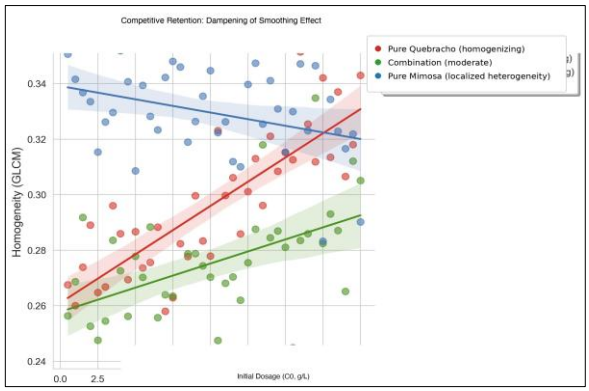


Figure 9. Mixed-system retention behavior: dampening of the image-based surface-regularity trend.

4. Discussion

Gravimetric retention, texture descriptors and Delta E00 together provide a coherent empirical framework for comparative retanning assessment. First, increasing C0 increased measurable dry weight gain. Second, surface-image texture metrics demonstrated that different systems translate deposition into distinct two-dimensional morphology outcomes, namely increased image regularity versus localized image heterogeneity. Third, color measurements indicated that higher mass retention did not necessarily increase initial color difference within the tested range (Figure 10).

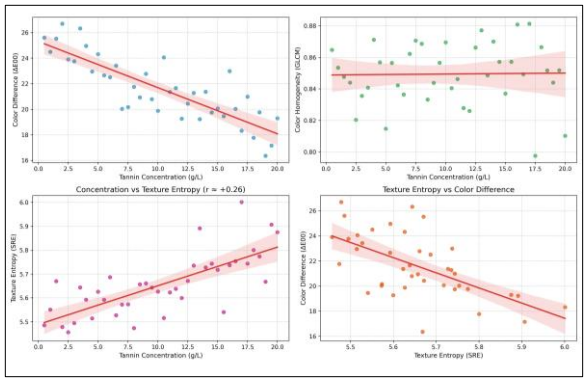


Figure 10. Chemical-visual correlation analysis for Mimosa-treated samples.

From an industrial-practice perspective, increased two-dimensional image homogeneity may be theoretically consistent with more uniform surface deposition, reduced visible grain irregularity and a more compact visual grain pattern, which can accompany perceived fullness when retanning agents distribute more evenly through the collagen network. However, this interpretation remains a process-level hypothesis in the present empirical framework; without ISO 2420 apparent-density or mass-per-unit-area data, ISO 3380 shrinkage temperature, thickness/compression measurements or cross-sectional microscopic validation, two-dimensional image homogeneity cannot be used as direct proof of bulk fullness or fiber compaction.

However, the proposed framework should be positioned as a low-cost and image-based screening tool rather than a replacement for established process-validation methods. Near-infrared spectroscopy combined with chemometric methods such as PCA has been shown to support non-destructive quality evaluation and process control in leather systems, and hyperspectral imaging combined with chemometrics has also been reported for leather identification and classification (Braz et al., 2018; Hou et al., 2023; Florio et al., 2025). The present approach may therefore be most useful as a complementary method in settings where rapid imaging is available but spectroscopic equipment or bath analytics are limited.

Correlation analysis further supports this integrated view: weight gain was positively associated with texture entropy in selected dosage-driven systems, indicating that increased deposition can be accompanied by measurable two-dimensional surface-image heterogeneity depending on tannin-pH conditions (Figure 11). These correlations describe image response and should not be extrapolated to bulk properties or three-dimensional roughness without shrinkage temperature, thickness, apparent density, compression-resilience, profilometry or calibrated microscopy validation.

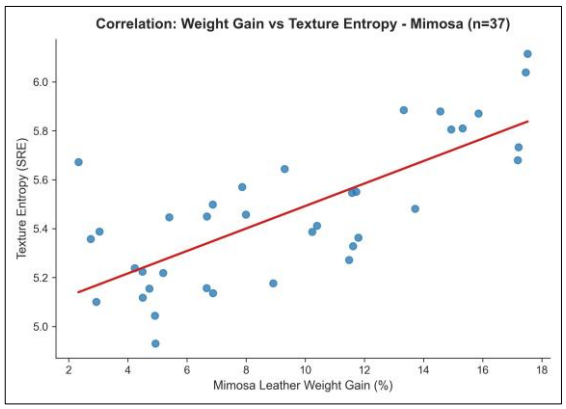


Figure 11. Correlation between leather weight gain (%) and texture entropy (SRE).

4.1 Limitations and Future Validation

A primary limitation is that tannin uptake was quantified exclusively by gravimetric dry mass retention. The equilibrium bath concentration (Ce) was not measured, and UV-VIS spectrophotometry was not used to track residual tannins in the bath solution. Consequently, the fitted functions are empirical dose-response curves versus initial dosage (C0), not thermodynamic adsorption isotherms. This distinction is important because classical isotherm parameters require equilibrium concentration data and should not be inferred from C0-based gravimetric trends alone.

A second limitation is the absence of shrinkage temperature (Ts) data. Ts is a key baseline indicator of tanning stability, and without it, gravimetric mass retention cannot distinguish chemical stabilization from physical deposition or filling. Therefore, this study evaluates mass retention and surface response rather than proving tanning efficacy. Future validation should include Ts measurements at representative dosage points, especially near apparent plateau regions.

A third limitation is that ISO-based physical validation was not performed. Apparent density, mass per unit area, thickness increase, compression-resilience and related measurements would be required to validate any bulk fullness interpretation. Accordingly, all fullness-related interpretations were removed or restricted to surface-level terminology.

A fourth limitation concerns image reproducibility. Although imaging conditions were standardized and GLCM displacement vectors were defined, pixel-to-mm calibration was not available in the dataset. Future studies should report magnification, spatial calibration, illumination geometry, camera settings and sensitivity analyses across ROI selections, because GLCM descriptors depend on acquisition and preprocessing parameters. Three-dimensional profilometry or calibrated digital microscopy should also be used to connect image descriptors with physical roughness metrics such as Ra or Rq.

Finally, CIEDE2000 (Delta E00) was retained for comparability with established leather and industrial color-difference literature. Future studies should include CAM16-UCS-based calculations, replicate batches and accelerated lightfastness or aging tests to determine whether the same initial color-consistency trends are preserved over time.

5. Conclusion

This study established a comparative, low-cost empirical screening framework for evaluating vegetable retanning behavior in wet-blue leather by integrating gravimetric mass retention, image-derived surface texture descriptors and colorimetric measurements. Because the equilibrium bath concentration was not monitored, tannin deposition was interpreted through dry weight gain as a function of the applied initial dosage, and the fitted curves were treated only as empirical dose-response relationships. Because equilibrium bath concentration was not measured, the reported mass-retention curves define only a descriptive initial-dosage trend boundary rather than calibrated bath-exhaustion behavior; future studies should combine gravimetry with UV-VIS spectrophotometry or high-performance liquid chromatography (HPLC) to quantify residual tannin concentrations.

The results showed clear pH-dependent differences among the retanning systems. Quebracho at pH 4.0 showed a bounded response associated with increased image-based surface regularity, whereas mimosa at pH 5.5 showed continued mass accumulation accompanied by localized image-texture heterogeneity. These findings indicate that tannin type and pH influence the way

retained material is expressed in two-dimensional surface images; however, the results should not be interpreted as direct evidence of bulk fullness, physical roughness reduction or tanning stabilization.

Within the investigated dosage range, increased gravimetric retention did not necessarily increase initial color difference. Mimosa showed comparatively lower initial color difference at both pH levels, whereas the binary mixture produced intermediate and less consistent responses. The color findings should therefore be interpreted as comparative initial color-consistency trends within the present measurement framework, not as evidence of lightfastness or long-term initial color consistency.

Overall, the combined use of gravimetric retention, GLCM-derived descriptors, SRE and color-difference analysis provides a practical, low-cost, non-destructive screening strategy for comparative retanning evaluation. Future studies should strengthen this framework by adding certified tannin specifications, UV-VIS bath exhaustion monitoring, equilibrium bath concentration measurement, shrinkage temperature measurement, standardized physical testing, calibrated three-dimensional or microscopic surface validation, spectroscopic or hyperspectral benchmarking and modern perceptual color-space validation.

Author Contributions

The author's contribution percentages are presented below. The author reviewed and approved the final version of the manuscript.

	Ş.Ö.
C	100
D	100
DCP	100
DAI	100
L	100
W	100
CR	100
SR	100
PM	100

C= concept, D= design, S= supervision, DCP= data collection and/or processing, DAI= data analysis and/or interpretation, L= literature search, W= writing, CR= critical review, SR= submission and revision, PM= project management.

Conflict of Interest

The author declared that there is no conflict of interest.

Ethical Consideration

Ethics committee approval was not required because the study did not involve animals or humans.

Acknowledgements

The author acknowledges the laboratory facilities and technical support provided during the experimental work. No specific external funding was declared for this study.

References

Balasubramanian, P., Ramalingam, S., & Rao, J. R. (2017). Detritus to functional auxiliary: Twin properties polymer from woody biomass for leather post-tanning application. *ACS Sustainable Chemistry & Engineering*, *5*(8), 7020–7029. https://doi.org/10.1021/acssuschemeng.7b01254

Baraldi, A., & Parmiggiani, F. (1995). An investigation of the textural characteristics associated with gray level cooccurrence matrix statistical parameters. *IEEE Transactions on Geoscience and Remote Sensing*, *33*(2), 293–304. https://doi.org/10.1109/TGRS.1995.8746010

Basova, O., Gladilin, S., Kokhan, V., Kharkevich, M. V., Sarycheva, A., Konovalenko, I., Chobanu, M. K., & Nikolaev, I. P. (2024). Evaluation of color difference models for wide color gamut and high dynamic range imaging. *Journal of Imaging*, *10*(12), Article 317. https://doi.org/10.3390/jimaging10120317

Bbumba, S., Karume, I., Nsamba, H. K., Kigozi, M., & Kato, M. (2024). An insight into isotherm models in physical characterization of adsorption studies. *European Journal of Applied Sciences*, *12*(2), 115–134. https://doi.org/10.14738/aivp.122.16738

Braz, C. E. M., Jacinto, M. A. C., Pereira-Filho, E. R., Souza, G. B., & Nogueira, A. R. A. (2018). Potential of near-infrared spectroscopy for quality evaluation of cattle leather. *Spectrochimica Acta Part A: Molecular and Biomolecular Spectroscopy*, *202*, 182–186. https://doi.org/10.1016/j.saa.2018.05.025

Covington, A. D., & Wise, W. R. (2019). *Tanning chemistry: The science of leather* (2nd ed.). Royal Society of Chemistry. https://doi.org/10.1039/9781839168826

Florio, C., Medici, A., Aveta, R., Esposito, L., Favazzi, A., Belvedere, F., Zarrelli, A., & Sarno, M. (2025). The potential of near infrared (NIR) spectroscopy coupled to principal component analysis (PCA) for product and tanning process control of innovative leathers. *Scientific Reports*, *15*, Article 35795. https://doi.org/10.1038/s41598-025-17598-7

Haralick, R. M., Shanmugam, K., & Dinstein, I. (1973). Textural features for image classification. *IEEE Transactions on Systems, Man, and Cybernetics*, *SMC-3*(6), 610–621. https://doi.org/10.1109/TSMC.1973.4309314

Hou, Q., Li, M., Han, Q., Yang, N., & Cheng, Y. (2023). Spectral characterization and identification of natural and regenerated leather based on hyperspectral imaging system. *Coatings*, *13*(2), Article 450. https://doi.org/10.3390/coatings13020450

International Organization for Standardization. (2015). *Leather — Physical and mechanical tests — Determination of shrinkage temperature up to 100 °C* (ISO Standard No. 3380:2015). https://www.iso.org/standard/60822.html

International Organization for Standardization. (2017). *Leather — Physical and mechanical tests — Determination of apparent density and mass per unit area* (ISO Standard No. 2420:2017). https://www.iso.org/standard/68314.html

Li, C., Li, Z., Wang, Z., Xu, Y., Luo, M. R., Cui, G., Melgosa, M., Brill, M. H., & Pointer, M. (2017). Comprehensive color solutions: CAM16, CAT16, and CAM16-UCS. *Color Research & Application*, *42*(6), 703–718. https://doi.org/10.1002/col.22131

Luo, M. R., Xu, Q., Pointer, M., Melgosa, M., Cui, G., Li, C., Xiao, K., & Huang, M. (2023). A comprehensive test of colour-difference formulae and uniform colour spaces using

available visual datasets. *Color Research & Application*, *48*(3), 267–282. https://doi.org/10.1002/col.22844

Nurichsanto, Y., Pertiwiningrum, A., Fitriyanto, N. A., & Pastawan, V. (2023). The effect of storage time on physical quality of vegetable tanned goat leather. *Advances in Biological Sciences Research*, *77*, 77–83. https://doi.org/10.2991/978-94-6463-116-6_11

Qiu, H., Lv, L., Pan, B., Zhang, Q., Zhang, W., & Zhang, Q. (2009). Critical review in adsorption kinetic models. *Journal of Zhejiang University SCIENCE A*, *10*(5), 716–724. https://doi.org/10.1631/jzus.A0820524

Raggi, A., & Barbiroli, G. (1993). Colour-difference measurement: The sensitivity of various instruments compared. *Color Research & Application*, *18*(1), 11–27. https://doi.org/10.1002/col.5080180105

Sabeenian, R. S., & Dinesh, P. M. (2011). Texture image classification using gray level weight matrix (GLWM). *Communications in Computer and Information Science*, *263*, 263–266. https://doi.org/10.1007/978-3-642-20573-6_43

Varghese, A., Jain, S., Prince, A. A., & Jawahar, M. (2020). Digital microscopic image sensing and processing for leather species identification. *IEEE Sensors Journal*, *20*(17), 10045–10056. https://doi.org/10.1109/JSEN.2020.2991881

Venter, P., Senekal, N. D., Amra-Jordaan, M., Bonnet, S. L., & van der Westhuizen, J. H. (2012). Analysis of commercial proanthocyanidins. Part 2: An electrospray mass spectrometry investigation into the chemical composition of sulfited quebracho heartwood extract. *Phytochemistry*, *78*, 156–169. https://doi.org/10.1016/j.phytochem.2012.01.027

Wilson, D., Tsigkou, O., Bosworth, L. A., & Jones, C. (2023). Leather-like materials by cellular agriculture. *Textile Progress*, *55*(1), 1–45. https://doi.org/10.1080/00405167.2023.2188835